A Miniaturized Absorptive Frequency Selective Surface

Qiang Chen, Jiajun Bai, Liang Chen and Yunqi Fu, *Member, IEEE*

***Abstract*—A miniaturized absorptive frequency selective surface (MAFSS) is presented in this paper, composed of a layer of miniaturized resistive surface placed above a metallic band-pass FSS. The MAFSS performs as a bandpass filter at operation band around 0.92GHz, and acts as an absorber over a wide out of band 3-9GHz. Moreover, due to its miniaturized elements, the MAFSS exhibits the property of eliminating the grating lobe in absorption band when illuminated by oblique incident wave. Numerical and experimental results have been given.**

***Index Terms*—Frequency Selective surface, Miniaturized elements, RCS.**

I. Introduction

DESIGN of stealthy radome has attracted growing attention in the stealthy aircraft application because the radar system is usually a strong scattering source [1], [2]. Generally, an ideal stealthy radome should effectively reduce the radar cross section (RCS) of the antenna system, and meanwhile ensure its normal operation without distorting the radiation performance. An approach is to use bandpass Frequency selective surface (FSS) in the design of stealthy radome [3]-[5]. Such radome could reflect the out-of-band incoming waves to other direction resorting to the conformal shape, thus reducing the monostatic RCS, While the operation signal is allowed to pass through the radome normally. However, its bistatic RCS might be increased due to the reflection.

In the past twenty years, another concept of absorptive FSS (AFSS), which is also transmissive at a given frequency, has been proposed and investigated [6]-[10]. It absorbs rather than reflecting the out-of-band waves, reducing bistatic RCS as well. The concept was firstly presented in an US patent in 1995 [6]. About a couple of ten years later, a layered AFSS structure with a good absorptive/transmissive property was designed [7]. It is composed of a metallic bandpass FSS and a periodic resistive surface. Some design principles were also discussed.

This work was supported by Program for New Century Excellent Talents in University under grant NO. NCET-10-0894

.Qiang Chen, Jiajun Bai, Liang Chen and Yunqi Fu, are with the College of Electronic Science and Engineering, National University of Defense Technology, Changsha, 410073, China. (yunqifu@nudt.edu.cn)

In our previous work, another AFSS structure was designed and fabricated [9]. Its absorptive /transmissive property was numerically and experimentally verified. The AFSS was later applied as a planar stealthy radome for a microstrip antenna [10]. When illuminated by an oblique incident plane wave, it could effectively reduce the bistatic RCS. However, when the mono-static reflection of oblique incidence is further studied, grating lobe problem should be noticed. Grating lobe would cause undesirable increase of mono-static RCS if it appeared in the direction close to the incident wave and could not be effectively absorbed. Once the backward grating lobe appears in the designed absorption band, the stealthy performance of the AFSS radome would be distorted.

One approach to the grating lobe problem is to employ miniaturized elements in AFSS structure, so the frequency of grating lobe would be shifted to higher frequencies, out of the absorption band. Therefore, both the monostatic and bistatic RCS of the miniaturized AFSS (MAFSS) would be effectively reduced over the absorption band. In this paper, firstly the grating lobe problem of the AFSS presented in [10] is discussed. Then a MAFSS structure has been designed and fabricated to this problem. Its absorptive/transmissive property has been numerically and experimentally verified. Above all, its efficiency of eliminating the grating lobe in the absorption band has been validated.

II. Grating lobe problem

Considering a one-dimensional periodic structure with inter-element spacing D is illuminated by a plane wave with oblique incident angle η, as depicted in Fig.1, a grating lobe may exist in the direction η_g .

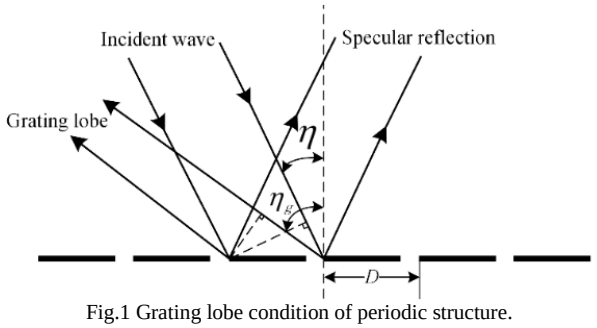

Fig.1 Grating lobe condition of periodic structure.

Grating lobe condition is given by [3]:

$$\beta D(\sin\eta + \sin\eta_g) = 1 \tag{1}$$

Where $\beta = \frac{2\pi}{\lambda_g}$,

Thus the frequency of grating lobe is

$$f_g = \frac{c}{\lambda_g} = \frac{nc}{D\left(\sin\eta + \sin\eta_g\right)} \quad (c = 3\times10^8 m/s) \qquad (2)$$

For a planar periodic structure, specular reflection and first-order grating lobe (n=1) is the main scattering. When the grating lobe appears in the backward direction $(\eta_g \approx \eta)$, the backscattering will cause undesirable increase of monostatic RCS. If it could not be effectively absorbed over the absorption band, the absorptive performance would be discounted.

The AFSS presented in [10] faces with the grating lobe problem. The periodicity of the unit cell on the top resistive layer is 36mm, and its absorption band is designed to be 3-9GHz. From eq. (2), considering the incident angle $\eta = 30°$, the grating lobe in the backward direction appears in the frequency 8.33GHz, just in the absorption band. In Fig.2, the bistatic reflection of a finite AFSS with dimensions of 216mm×216mm at several frequencies is analyzed by Ansoft HFSS, together with that of a metal sheet with the same dimensions. It can be seen that the specular reflection is reduced in each case due to the absorptive property, while in the backward direction the monostatic reflection is increased due to the grating lobe around the frequency 8.33GHz.

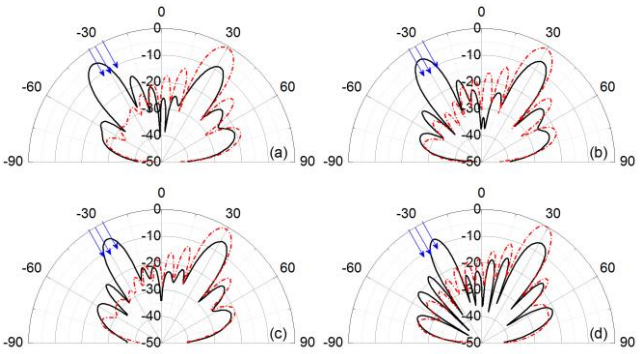

Fig.2 Simulated bistatic reflection of a finite AFSS (solid line) and a metal sheet (dotted line) at oblique incidence. Incident angle: 30deg; polarization: TM. (a) 7.625GHz; (b) 8.1GHz; (c) 8.575GHz; (d) 9.05GHz.

From eq. (2), the frequency of grating lobe is inversely proportional to the periodicity *D*. A solution to this problem is to employ miniaturized elements, so that the grating lobe would be shifted to the frequency above the absorption band. Supposing the upper frequency of the designed absorption band is f_H, to avoid the grating lobe in the absorption band, the frequency of the grating lobe $f_{g\min}$ should be greater than f_H:

$$f_{g\min} = \frac{c}{D_{\max}\left(\sin\eta + \sin\eta_g\right)} \geq f_H, \qquad (3)$$

Then the periodicity of the top layer of the AFSS structure should be:

$$D_{\max} \leq \frac{c}{f_H\left(\sin\eta + \sin\eta_g\right)} = \frac{\lambda_H}{\sin\eta + \sin\eta_g} \leq \frac{\lambda_H}{\sin\eta + 1} \qquad (4)$$

III. Structure Design and Discussion

A MAFSS structure whose periodicity determined by eq. (4) is designed to avoid grating lobe in the absorbing band when illuminated by oblique incident wave. The transmission frequency is designed to be around 0.92GHz and the absorption band is 3-9GHz.

A three-dimensional configuration of the MAFSS is shown in Fig. 3 (a). It is composed of a layer of resistive surface on the top and a bandpass FSS at the bottom, separated by a PMI foam (Polymethacrylimide) with $\varepsilon_r \approx 1$. The bandpass FSS is designed to transmit the in-band signals and the resistive surface is used to absorb the wide out-of-band waves with the bandpass FSS as a ground plane. The resistive surface consists of a two-dimensional periodic arrangements of incurved square loop (ISL) loaded with lumped resistors, as shown in Fig.3 (b). The bandpass FSS consists of two layers of metallic patches on the two sides of a thin dielectric layer. The Unit cells of both layers are illustrated in Fig. 3 (c)-(d).

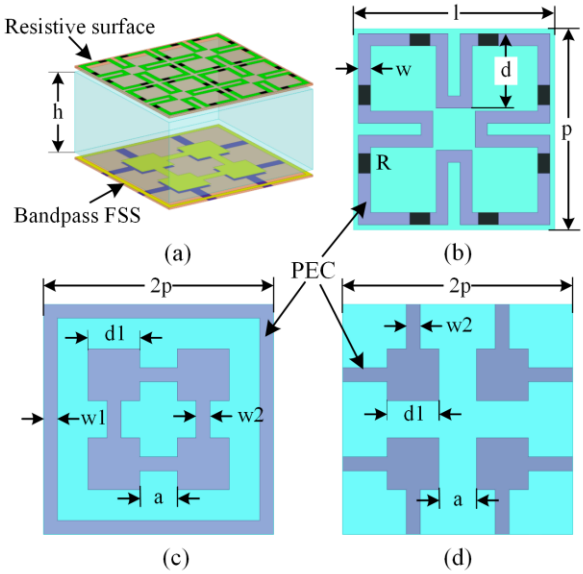

Fig.3 unit cell geometries of the MAFSS structure.

The geometrical parameters of the unit cells of both layers are summarized in Table I, all optimized by Ansoft HFSS. The resistance R loaded in the ISL is one of the key parameters affecting the absorptive property of the MAFSS. It is optimized to be 120Ω.

TABLE I
DIMENSIONS OF THE UNIT CELLS OF THE MAFSS (mm)

h	p	l	w	d	a	w1	d1	w2
10	10	9.5	0.6	3.7	1.62	1.21	4.5	1.21

Because the incurved structure increases the equivalent

inductance of the square loop, the periodicity of the ISL is miniaturized to be only 10mm, $0.3\lambda_H$ at the higher frequency of the absorption band (9GHz). The unit size of the bandpass FSS is 20mm, which is miniaturized by increasing the distributed capacitance between the two metallic patches in different layers [11]. It is characterized by a pass band around 0.92GHz and a large rejection band of 1.5-12GHz.

The simulated reflection and transmission coefficients of the MAFSS for normal incidence are shown in Fig 4. The reflection is obtained by exciting plane wave on the resistive side of the MAFSS. The insertion loss is less than 0.5dB around 0.92GHz and the absorption band is over 2.8-9GHz.

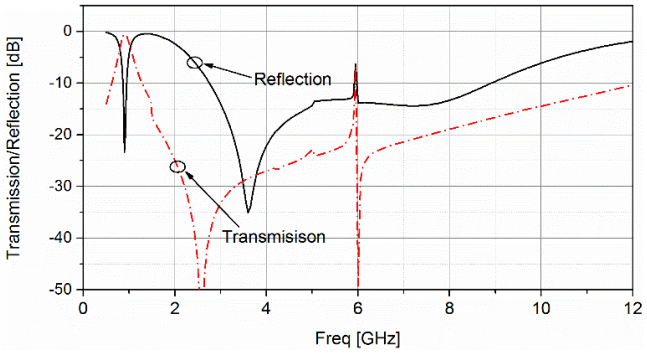

Fig.4 Simulated reflection and transmission coefficients of the MAFSS.

Furthermore, in Fig.5 the simulated bistatic reflections of a finite MAFSS and a metal sheet at different frequencies are shown for the 30° oblique incident wave. Their dimensions are both 200mm×200mm (a larger dimension is hard to be modeled and simulated on our server HP Proliant DL580G7 due to the complex structure of the MAFSS). It can be seen that in the whole space the bistatic reflection of the MAFSS is reduced for its absorption property, especially in the specular direction. What's more, in the backward direction, there is no grating lobe as we discussed in Section Ⅱ.

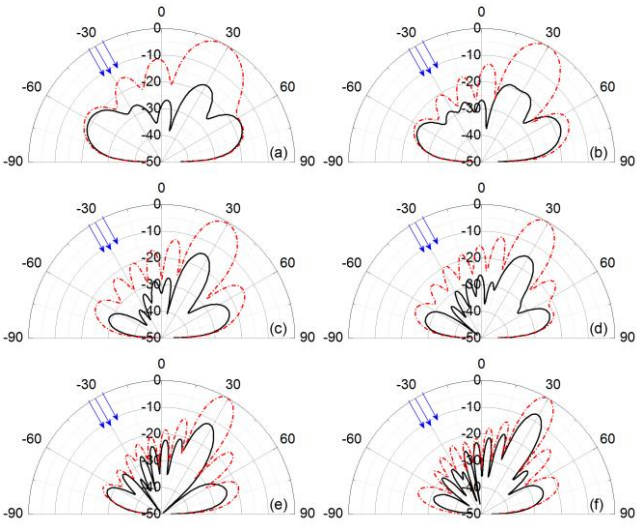

Fig.5 Simulated bistatic reflection of a finite MAFSS (solid line) and a metal sheet (dotted line) at oblique incidence. Incident angle: 30deg; polarization: TM. (a)4GHz; (b) 5GHz; (c)6GHz; (d) 7GHz; (e) 8GHz; (f) 9GHz.

IV. Experimental Results

The performance of the transmission and absorption of the MAFSS and its efficiency on eliminating grating lobe are experimentally demonstrated using a free-space measurement setup. A finite sample of the MAFSS, with the dimensions of 300mm×300mm, is designed and fabricated, as depicted in Fig.6. There are 30×30 ISL cells on the top resistive layer and 15×15cells at the bottom bandpass layer. Both the resistive layer and bandpass FSS layer are printed on thin F_4BM substrate with $\varepsilon_r = 2.25$ and thickness 0.25mm.

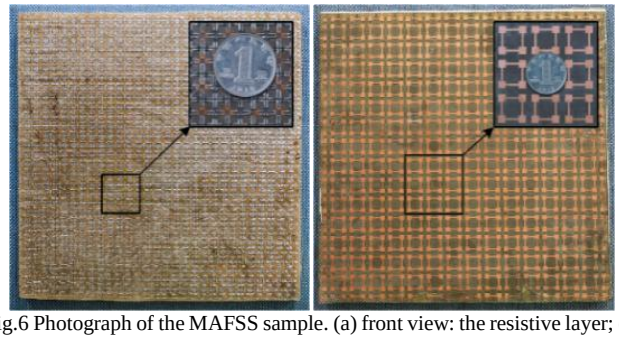

Fig.6 Photograph of the MAFSS sample. (a) front view: the resistive layer; (b) back view: the bandpass layer.

Firstly, the transmission property of the MAFSS sample was investigated. A wooden fixture with a square window at its center was built. It is covered with RF absorber to absorb the background waves. The fixture with the MAFSS sample embedded in the window was placed between two double-ridged horn antennas ETS 3115 connected to a vector network analyzer Agilent N5230C. The operation band of the horn antenna is 1-18GHz, but still has 3dB gain at frequency down to 0.75GHz. To ensure the sample is excited with plane wave, it was placed in the far field of the horn antenna.

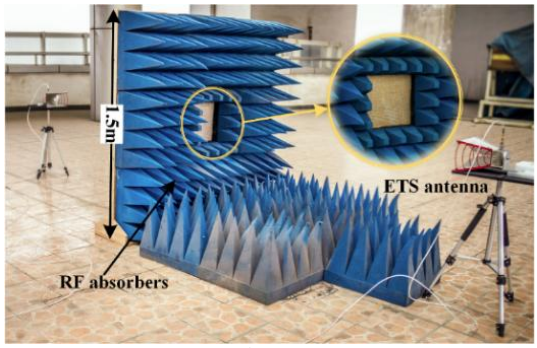

Fig.7 Photograph of the measurement setup.

Fig. 7 shows a photograph of the measurement setup. Electromagnetic waves radiated from the horn antenna illuminates on the resistive side of the MAFSS for different oblique incident angles. The transmission coefficient between the two antennas was measured. The result is calibrated by that of the wooden fixture without MAFSS sample, as shown in Fig.8, along with the simulated results. Experimental results agree well with the simulation. The transmission band is around 0.92GHz, nearly independent of the incidence angle within ±30° , the insertion loss is less than 0.5dB. The

disagreement at the lower frequency is probably due to the fabrication error and the measurement situation.

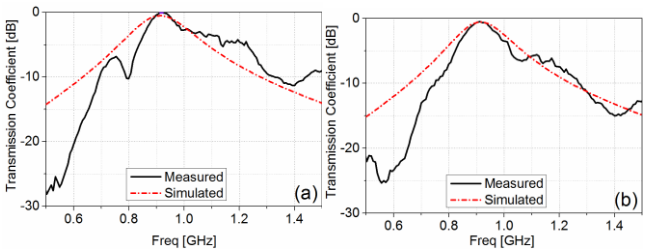

Fig.8 Measured and simulated transmission coefficient of the MAFSS. Polarization: TM. (a) 15deg, (b) 30deg.

Secondly, the absorption property of the MAFSS sample was studied. The two antennas were placed symmetrically both on the resistive side of the MAFSS sample to measure the bistatic reflection. The measured bistatic reflection coefficients of the MAFSS sample for oblique incidence is calibrated by that of a metal sheet with the same dimensions, as shown in Fig.9, together with the simulated results. Wideband absorption for both TE and TM polarization can be observed.

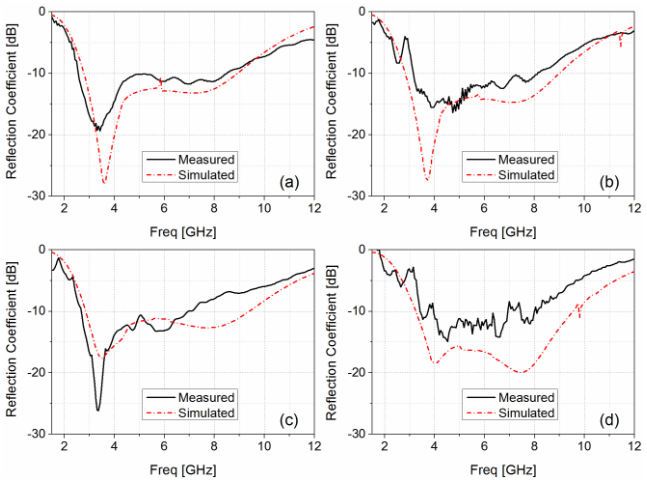

Fig. 9 Measured and simulated reflection coefficients of the MAFSS. (a) 15deg, TE; (b) 15deg, TM, (c) 30deg, TE; (d) 30deg, TM.

What's more, to validate the efficiency on the elimination of grating lobe, the backscattering (monostatic reflection) of the MAFSS sample for 30° oblique incidence was measured, compared with that of the AFSS in [10] and a metal sheet, all with the same dimensions. The measured results are shown in Fig. 10. It can be seen that the backscattering of the MAFSS, as expected, agrees well with that of the metal sheet in the whole absorption band, while in the range of 8-9GHz, there is an increase of the backscattering for the AFSS in [10] due to its first order grating lobe. It can be concluded that it is effective for the MAFSS to eliminate the grating lobe in absorption band by the miniaturized elements.

V. Conclusion

In this paper we have presented a MAFSS structure. The MAFSS is characterized by a good absorptive/ transmissive property. The transmission band is around 0.92GHz, with insertion loss less than 0.5dB, and the absorption band is 3-9GHz, respectively. Besides, due to the miniaturized elements, the MAFSS is experimentally and numerically certificated to be effective to eliminate the potential grating lobe (particularly in the backward direction) appeared in the absorption band when illuminated by oblique incident waves.

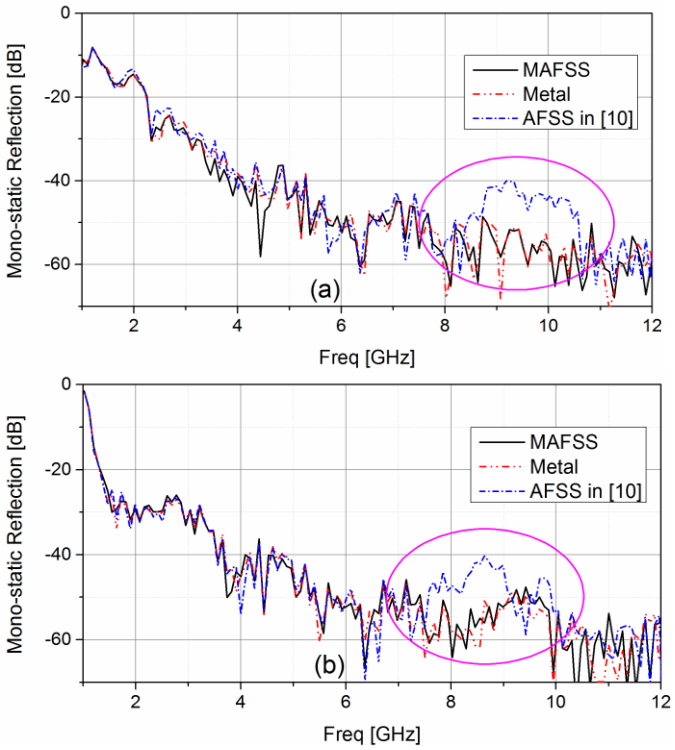

Fig.10 Measured backscattering of the MAFSS sample, the metal sheet and the AFSS in [10] for oblique incidence. Incident angle: 30deg; polarization: (a) TE, (b) TM.

References

[1] Y. C. Chang, "Low radar cross section radome", US Patent 6639,567 B2, Oct. 2003.

[2] D. J. Kozakoff, Analysis of radome-Enclosed Antennas. Norwood, MA: Artech House, 1997.

[3] B.A. Munk, *Frequency Selective Surfaces: Theory and Design*, New York: Wiley, 2000.

[4] X. Chen, Y. Q. Li, Y. Q. Fu, and N. C. Yuan, "Design and analysis of lumped resistor loaded metamaterial absorber with transmission band," *Optics Express*, vol. 20, pp. 28347-28352, 2012.

[5] B.A. Munk, *Metamaterials: critique and alternatives*, New York: Wiley, 2009, pp.61-70.

[6] W. S. Arceneaux, R. D. Akins and W. B. May, "Absorptive/transmissive radome," US Patent 5,400,043, 1995.

[7] F. Costa and A. Monorchio, "A Frequency Selective Radome with Wideband Absorbing Properties," *IEEE Trans. Antennas Propag.*, vol. 60, no. 6, pp. 2740-2747, Jun. 2012.

[8] A. Motevasselian, B.L.G. Jonsson, "Design of a wideband rasorber with a polarization-sensitive transparent window," *IET Microw. Antennas Propag.*, vol. 6, pp. 747-755, 2012.

[9] L. G. Liu, P. F. Guo, J. J. Huang, W. W. Wu, J. J. Mo, Y. Q. Fu and N. C. Yuan, "Design of an invisible radome by metamaterial absorbers loaded with lumped resistors," *Chin. Phys. Lett.*, vol. 29, no. 1, 2012.

[10] Q. Chen, Y.Q. Fu, "A planar stealthy antenna radome using absorptive frequency selective surface," *Microw. Opt. Tech. Lett.*, vol.56, no.8, pp.1788-1792, 2014.

[11] F. Deng and X. G. Wu, "A novel miniaturized Frequency Selective Surface," in *Proc. 10th ISAPE*, Xi'an, 2012, pp. 377-380